Extreme Degree of Ionization in Homogenous Micro-Capillary Plasma Columns Heated by Ultrafast Current Pulses

G. Avaria,[1,5] M. Grisham,[1] J. Li,[1] F. G. Tomasel,[1,2] V. N. Shlyaptsev,[1] M. Busquet,[3] M. Woolston,[1] and J. J. Rocca[1,4,*]
[1]Department of Electrical and Computer Engineering, Colorado State University, Fort Collins, Colorado 80523, USA
[2]Advanced Energy Industries, Fort Collins, Colorado 80525, USA
[3]ARTEP Inc., Ellicott City, Maryland 21042, USA
[4]Department of Physics, Colorado State University, Fort Collins, Colorado 80523, USA
[5]Comisión Chilena de Energía Nuclear, Santiago, Chile
and Center for Research and Applications in Plasma Physics and Pulsed Power, P4, Casilla 188-D, Santiago, Chile
(Received 17 March 2014; published 5 March 2015)

Homogeneous plasma columns with ionization levels typical of megaampere discharges are created by rapidly heating gas-filled 520-μm-diameter channels with nanosecond rise time current pulses of 40 kA. Current densities of up to 0.3 GA cm^{-2} greatly increase Joule heating with respect to conventional capillary discharge Z pinches, reaching unprecedented degrees of ionization for a high-Z plasma column heated by a current pulse of remarkably low amplitude. Dense xenon plasmas are ionized to Xe^{28+}, while xenon impurities in hydrogen discharges reach Xe^{30+}. The unique characteristics of these hot, ~300:1 length-to-diameter aspect ratio plasmas allow the observation of unexpected spectroscopic phenomena. Axial spectra show the unusual dominance of the intercombination line over the resonance line of He-like Al by nearly an order of magnitude, caused by differences in opacities in the axial and radial directions. These plasma columns could enable the development of sub-10-nm x-ray lasers.

DOI: 10.1103/PhysRevLett.114.095001 PACS numbers: 52.58.Lq, 42.55.Vc, 52.50.Nr, 52.59.Ye

The generation of hot, dense plasma columns using compact setups is a difficult problem of significant interest for extending tabletop soft x-ray lasers to shorter wavelengths [1], creating plasma waveguides [2,3] with high-Z ions [4], generating neutrons [5], and performing fundamental plasma studies. Pulsed electrical discharges are the simplest method to produce hot and dense plasma columns. One of the most studied pulsed-power schemes is the Z-pinch discharge, where plasmas are created by converting the kinetic energy of an electromagnetically driven imploding cylindrical sheath into thermal energy [6]. While conceptually simple, the creation of dense Z-pinch plasmas with electron temperatures of several hundred eV typically requires megaampere-level currents [7]. Moreover, nonuniform compressions and large-scale instabilities characteristic of these high-current Z pinches limit their use in applications requiring highly homogeneous columns. However, the recent development of Z-pinch discharges confined by 3–4-mm-diameter capillary channels driven by moderately fast current pulses (20–50 ns rise time) has enabled the generation of dense plasma columns of remarkable uniformity with electron temperatures of up to 150 eV [8] meeting the demanding stability requirements of gain-saturated soft x-ray lasers [9,10]. These discharge-based lasers are capable of generating powerful 46.9 nm wavelength laser beams with essentially full spatial coherence [11] that the presence of instabilities would readily destroy [12]. Capillary discharges driven by 200 kA current pulses have been shown to produce plasmas with temperatures in excess of 250 eV [13,14]. However, producing yet higher temperatures proves to be challenging. Analysis of the energy balance for these discharges excited by current pulses with tens of nanoseconds rise time shows that only a small fraction of the energy initially stored is used to heat the imploded column; much of the energy goes into radially accelerating the plasma, and is not efficiently transformed into thermal energy at the core. For example, in the Ar capillary discharge soft x-ray laser experiments of Refs. [9–11,15] only 0.5% of the driver's available energy is converted into thermal energy at the core. This intrinsic limitation of the kinetic conversion scheme makes it difficult to extend it to applications such as the development of sub-10-nm wavelength lasers, which require axially uniform plasma columns that are significantly denser and hotter (e.g., 26 times ionized Xe [16,17] and an electron temperatures of ~400 eV). Such scaling is particularly challenging for high-Z plasmas where radiative cooling is large [5].

In this Letter we demonstrate that Joule heating of gas-filled micro-capillary channels with ultrafast current pulses of nanosecond rise time and unusually low amplitude efficiently generates hot plasma columns with extreme degrees of ionization. Xenon discharges in 520-μm-diameter capillary channels heated by ~4 ns rise time current pulses of 35–40 kA peak amplitude reached Xe^{28+}, while ionization of Xe impurities in H_2 discharges reached Xe^{30+} [Fig. 1(a)]. This unprecedented degree of ionization for a high-Z plasma column heated by a low amplitude current pulse is obtained despite the transient

nature of the discharge that creates ion population distributions far from steady state. Spectra from these plasmas agree with those synthesized from simulations predicting on-axis electron temperatures up to $T_e \sim 0.7$ keV. We show that contrary to the case of conventional capillary discharge Z pinches, the dominant plasma heating source in this ultrafast micro-capillary discharge regime is Joule heating. The decrease in channel diameter increases the current density up to 0.3 GA cm^{-2}, allowing us to reach temperatures several times higher than those of conventional capillary discharges excited with similar peak currents. This new approach reduces by nearly an order of magnitude the current necessary to heat dense homogeneous plasma columns: simulations suggest current pulses of ~0.5 MA are required to reach similar ionization in 4-mm-diameter capillary discharges. In addition, the short current pulse keeps the power load to the wall at the same levels encountered in previous capillary discharges [10,15]. Although a number of micro-capillary discharges have been previously studied [3,18–25], these discharges had either much longer excitation pulses leading to large wall ablation and cold plasmas, e.g., electron temperatures $T_e \sim 10$ eV for a 500 kA current pulse of 300 ns duration in a 20-μm-diameter capillary [20], or nanosecond duration but power density depositions orders of magnitude lower than those of interest here, resulting in $T_e \sim 30$ eV [24,25]. The results presented herein show for the first time that high-aspect-ratio plasma columns (~300:1 length to diameter) with extreme degrees of ionization and temperatures of several hundred eV can be generated by modest current pulses in compact discharge devices. The micro-capillary geometry is also well suited to achieve, through preionization, the highly uniform initial plasma conditions crucial for a stable radial collapse of the plasma column.

Figures 1(b)–1(f) show the results of hydrodynamic simulations conducted with a version of our code RADEX [26] designed to model capillary plasmas including transient atomic physics computed using data from the HULLAC code [27]. The code calculates self-consistent radiation transport for several hundred thousand lines originating from more than 5000 levels of all possible ion stages, and wall ablation. The rapid Joule heating of micro-capillary channels leads to unusually high electron temperatures [Fig. 1(d)] and extreme degrees of ionization [Fig. 1(f)]. The kinetic energy of the column still contributes to heat the plasma core, but it is not the overwhelmingly dominant heat source [28]. Simulations also show that ablation and ionization of wall material creates a peripheral plasma that distributes the electric current over the entire capillary diameter [see the integrated radial current profile in Fig. 1(c)]. The low fraction (5%–15%) of the total current flowing through the final compressed core contributes to slow down the growth of instabilities. Yet, the core is efficiently heated by high current densities of up to

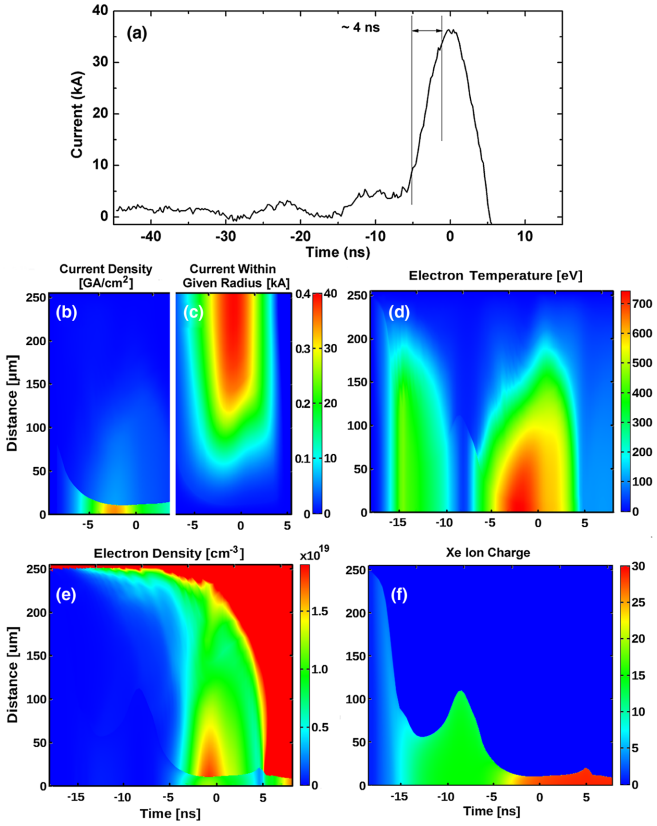

FIG. 1 (color online). (a) Current pulse used to excite 520-μm-diameter micro-capillary channels. A 3–5 kA prepulse consisting of a few oscillations lasting ~30 ns is followed by an ultrafast current pulse with a 3.8 ns (10%–90%) rise time above the prepulse. (b)–(f) Simulated evolution of current distribution and the plasma parameters in a 0.5 Torr, 80:1H_2:Xe mixture excited by a current pulse of 39.6 kA peak amplitude. The sharp boundaries in (b), (e), and (f) reflect the interface between the gas fill and the wall ablated material.

0.3 GA cm^{-2} [Fig. 1(b)], exceeding by an order of magnitude the simulated current density in 4-mm-diameter capillary discharges heated by 0.5 MA current pulses. Injection of ultrafast current pulses (10%–90% current rise time of 4 ns) of 39.6 kA amplitude into 520-μm-diameter capillary channels filled with a 0.5 Torr, 80:1H_2:Xe mixture is computed to yield an electron temperature of $T_e \sim 0.7$ keV [Fig. 1(d)] and electron densities of 1–1.5 $\times 10^{19}$ cm^{-3} [Fig. 1(e)]. After the plasma density peaks, the temperature rapidly drops due to the intense radiation emitted by the high-Z ions and the fast expansion [Fig. 1(d)]. Simulations of similar micro-capillary discharges in a pure Xe capillary at a pressure of 0.5 Torr compute a temperature of $T_e \sim 350$ eV near the axis, where the electron density is 3×10^{19} cm^{-3} and highly charged ions such as Ni-like Xe (Xe^{26+}), Co-like Xe (Xe^{27+}), and Fe-like Xe (Xe^{28+}) are predicted to be present.

Experiments were conducted exciting 520-μm-diameter, 3.3-cm-long gas-filled alumina (99.8%) capillaries. The

discharge is driven by a pulsed power generator consisting of an eight-stage Marx bank followed by two stages of pulse compression [28]. The Marx bank charges a coaxial oil-filled capacitor that is subsequently discharged into a radial, oil-filled Blumlein transmission line through a SF_6-filled spark-gap. The capillary is located at the axis of the Blumlein line forming a low inductance geometry. This radial line is rapidly discharged across the capillary channel through a set of seven parallel SF_6-filled spark gaps uniformly distributed around its outer perimeter.

Increasing the current density by reducing the capillary diameter alone does not necessarily result in hotter plasmas, as the increased power load to the walls can result in higher mass ablation and lower temperatures. However, if the use of a microcapillary is accompanied by ultrafast high current excitation, plasma columns with very high electron temperatures can be created by current pulses of unusually low amplitude. Figure 1(a) shows a typical current pulse used in the experiments, measured with an air-core Rogowski coil. The column is preionized by a microsecond-long, ~20 A current pulse that enables a uniform compression. The main current pulse is configured to have a preheating prepulse of 3–5 kA amplitude and ~30 ns duration. The main current pulse rapidly rises above this pedestal with a 10%–90% rise time of 3.8–4 ns to reach amplitudes of up to ~40 kA. Gas is injected into the capillary prior to the discharge current pulse, and the pressure is dynamically monitored with a capacitive gauge. Time-resolved spectra of the discharge plasma in the 1.4–2 nm wavelength region are recorded end on using a 2° grazing incidence flat-field spectrometer equipped with a 600 lines/mm variable-spacing, gold-coated grating and a gated microchannel plate (MCP) and CCD detector.

Figure 2 shows a sequence of measured time-resolved on-axis spectra spanning 2.6 ns around the peak of the current pulse for a 0.5 Torr Xe discharge in a 520-μm-diameter capillary heated by a 37.6 ± 0.6 kA current pulse. The kiloampere prepulse plays an important role in achieving the extreme degree of ionization observed; it is computed to preionize the Xe plasma to $Z \sim 12$–15, depending on the initial gas pressure. Starting from this degree of ionization, the plasma is rapidly heated and further ionized by the main ultrafast current pulse that follows. Spectra acquired 0.4 ns after the peak of the current pulse show dominant Co-like Xe (Xe^{27+}) lines followed in intensity by lines of Ni-like Xe (Xe^{26+}). The measured spectra also show the presence of Fe-like Xe (Xe^{28+}) lines, in agreement with spectra from simulations that predict an electron temperature of 350 eV. This represents an unprecedented degree of ionization and temperature for a high-Z plasma column heated by a modest amplitude current pulse. The measured and

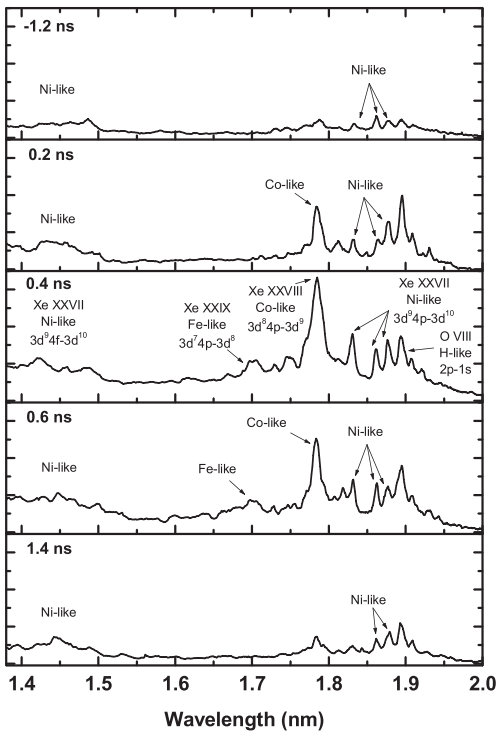

FIG. 2. Sequence of time-resolved single-shot spectra of Xe plasma in a 520-μm-diameter capillary channel excited by a 37.6 ± 0.6 kA current pulse. The Xe pressure was 0.5 Torr. Timing is referenced to the peak of the current pulse.

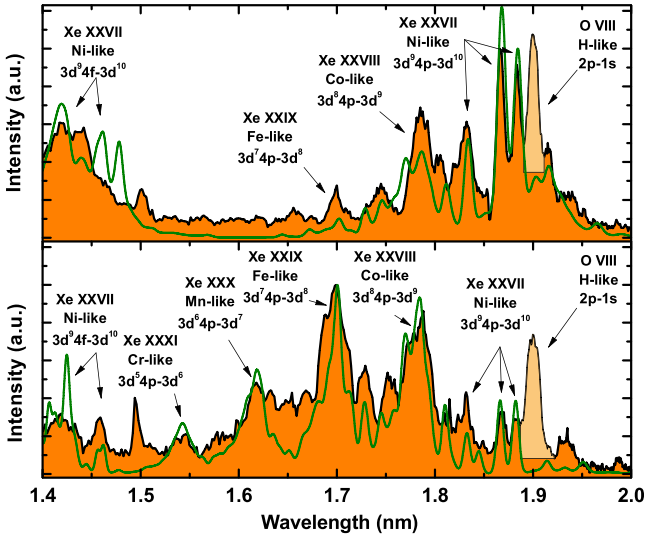

FIG. 3 (color online). Measured single-shot time-resolved spectra (solid area) and simulated spectra (green line) for discharge plasmas in a 520-μm-diameter capillary for two different conditions. (a) 4 Torr of Xe and peak discharge current 40.6 kA, 0.8 ns before the current pulse peak. Lines from Ni-like Xe (Xe^{26+}) and Co-like Xe (Xe^{27+}) dominate the spectra. The line at 1.9 nm is assigned to a blend of the $O^{7+}2p-1s$, Xe^{25+}, and Xe^{27+} lines. (b) 80:1 H_2:Xe mixture at 0.5 Torr and peak discharge current 39.6 kA, 1.2 ns before peak of current pulse. Line emission from Cr-like Xe (Xe^{30+}) is observed. The simulation does not include O impurities.

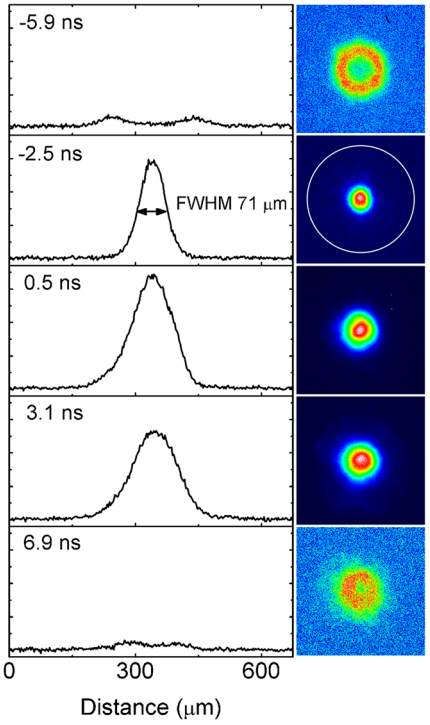

FIG. 4 (color online). Sequence of on-axis x-ray pinhole camera images illustrating the evolution of a Xe discharge in a 520-μm-diameter channel, heated by a 35.4 ± 0.9 kA current pulse. The time is referenced to the peak of the current pulse. The white contour represents the capillary wall. The temporal resolution is 2 ns and the spatial resolution is 42 μm.

simulated spectra of Fig. 3(a) show that a very high degree of ionization is maintained when the gas filling pressure is increased to 4 Torr. The simulated electron density in this case reaches $\sim 0.5 \times 10^{20}$ cm^{-3}. Plasma columns were also generated in microcapillaries filled with an $80:1\ H_2:Xe$ mixture. Figure 3(b) shows measured (solid area) and simulated (thin line) spectra of such plasma corresponding to a 0.5 Torr discharge in a 520-μm-diameter capillary. While the spectra are dominated by Fe-like Xe (Xe^{28+}) lines, lines from Mn-like Xe (Xe^{29+}) and Cr-like Xe (Xe^{30+}) are both predicted and observed. Simulations indicate that suprathermal, "hot" electrons play a secondary role in the measured high degree of ionization of the Xe plasma. Comparison of the time-gated experimental spectra with the transient atomic model simulations allowed us to evaluate their contribution. In the case of the pure Xe discharges both the relative amount of hot electrons (<0.3%) and their influence are small. Their role is computed to be larger in the $H_2:Xe$ mixture, increasing Z by 1–2 when the largest possible concentration of fast electrons is assumed.

Sequences of time-resolved, filtered soft x-ray pinhole images of the plasma column show symmetric compressions leading to plasma channels with a $\sim 300:1$ aspect ratio. Figure 4 presents a sequence of pinhole images for a

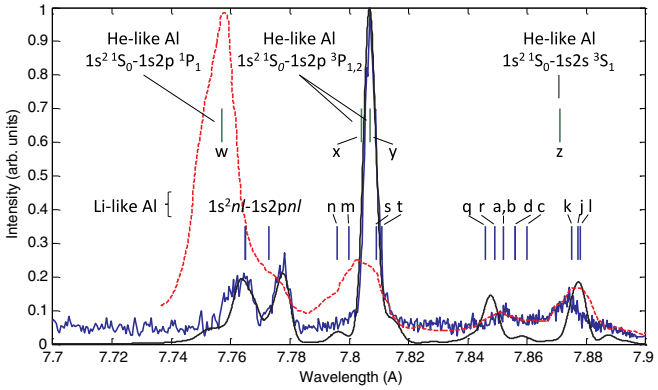

FIG. 5 (color online). Measured on-axis spectrum (blue) and simulated spectrum (black) of a neon discharge in a 520-μm-diameter alumina microcapillary showing the dominance of the $1s^2\ ^1S_0$-$1s2p\ ^3P_1$ intercombination line of He-like Al over the $1s^2\ ^1S_0$-$1s2p\ ^1P_1$ resonance line. The peak current was 36.0 kA and the neon pressure was 0.5 Torr. The dashed line spectrum, dominated by the resonant transition of He-like Al, is a typical spectrum from a laser-created Al plasma [30]. Nomenclature for the Li-like satellite lines follows Ref. [31].

0.5 Torr Xe discharge heated by current pulses of 35.4 ± 0.9 kA amplitude. The images were obtained by placing a 38-μm diameter pinhole at 14.6 cm from the capillary exit and acquired by a gated MCP and CCD detector with a magnification of 8.3×. The first image, taken 5.9 ns prior to the peak of the current pulse, shows a highly symmetric annular plasma shell. At this early stage in the compression the plasma is cold and practically no emission is observed at photon energies above 0.6 keV. This image was taken using a stacked Mylar-parylene foil filter (thicknesses of 1 and 0.1-μm, respectively), while later images used a Mylar-aluminum foil combination (thicknesses of 1 and 0.5-μm, respectively). The image taken 2.5 ns prior to the current peak shows emission at $h\nu > 0.6$ keV originating from a region ~ 70 μm in diameter centered at the capillary axis. The symmetry observed during the entire temporal evolution, including the stagnation and later expansion phase, suggests the column is free from major instabilities as in the case of larger diameter capillary discharges.

The unique characteristics of these plasma columns allow the observation of unexpected spectroscopic phenomena. As an example we discuss here the observation of the unusual dominance of the intercombination line intensity of He-like Al over the resonance line by nearly an order of magnitude in a Ne discharge in alumina microcapillaries (Fig. 5), where Al atoms originate from wall ablation. The strong dominance of the intercombination line originating from the $1s2p^3P_1$ level occurs despite it having a radiation decay probability several orders of magnitude smaller than of the resonance line originating from the $1s2p^1P_1$ singlet level. Model simulations rule out the possibility of this resulting from either recombination that preferentially populates the triplet levels, or from the excitation of these

levels by inner-shell electron impact ionization of Li-like ions. Also, in our case the anomaly cannot be attributed to the collisional mixing that affects the relaxation time during the expansion and cooling phase [29]. Instead, our simulations show that the cause of this effect is the very large aspect ratio geometry of the plasma, in which different optical depths in the transverse direction (optically thin for both lines) and longitudinal directions (optically thick for both lines) create a situation where the population of the $1s2p^3P_1$ level is favored over the $1s2p^1P_1$ upper level by up to 2 orders of magnitude, defining the line intensities in the axial direction.

The efficient generation of these highly ionized plasma columns using compact discharges opens a path to new applications of discharge-created plasmas. For example, the high density of Ni-like Xe ions combined with the rapid rise of the electron temperature can be expected to lead to strong monopole excitation of the $4d^1S_0$ level of Ni-like Xe resulting in a large transient population inversion and amplification in the $4d^1S_0$-$4p^1P_1$ line at $\lambda \sim 10$ nm. Our simulations predict that a fast rise of the temperature to >400 eV could result in transient gain of sufficient magnitude to produce a gain-saturated $\lambda \sim 10$ nm soft x-ray laser in plasma columns 5–7 cm in length. The unique characteristics of these plasma channels will also open new opportunities in fundamental plasma and atomic physics studies.

This work was supported by NSF Plasma Physics Grant No. PHY-1004295. We thank A. Faenov and F. B. Rozmej for helpful discussions. G. A. acknowledges the support from CONICYT PAI Inserción 791100020, PIA Anillo ACT 1115, and FONDECYT Iniciación 11121587.

*Corresponding author.
jorge.rocca@colostate.edu

[1] *X-Ray Lasers 2012*, edited by S. Sebban, J. Gautier, D. Ros, and P. Zeitoun (Springer, Heidelberg, 2013).
[2] C. G. Durfee and H. M. Milchberg, Phys. Rev. Lett. **71**, 2409 (1993).
[3] A. Butler, D. J. Spence, and S. M. Hooker, Phys. Rev. Lett. **89**, 185003 (2002).
[4] B. M. Luther, Y. Wang, M. C. Marconi, J. L. A. Chilla, M. A. Larotonda, and J. J. Rocca, Phys. Rev. Lett. **92**, 235002 (2004).
[5] C. L. Ruiz *et al.*, Phys. Rev. Lett. **93**, 015001 (2004).
[6] M. G. Haines, Plasma Phys. Controlled Fusion **53**, 093001 (2011).
[7] J. E. Bailey *et al.*, Phys. Rev. Lett. **92**, 085002 (2004).
[8] J. J. Rocca, O. D. Cortazar, B. Szapiro, K. Floyd, and F. G. Tomasel, Phys. Rev. E **47**, 1299 (1993).
[9] J. J. Rocca, V. Shlyaptsev, F. G. Tomasel, O. D. Cortazar, D. Hartshorn, and J. L. A. Chilla, Phys. Rev. Lett. **73**, 2192 (1994).
[10] B. R. Benware, C. D. Macchietto, C. H. Moreno, and J. J. Rocca, Phys. Rev. Lett. **81**, 5804 (1998).
[11] Y. Liu, M. Seminario, F. G. Tomasel, C. Chang, J. J. Rocca, and D. T. Attwood, Phys. Rev. A **63**, 033802 (2001).
[12] P. A. Amendt, M. Strauss, and R. A. London, Phys. Rev. A **53**, R23 (1996).
[13] J. J. Gonzalez, M. Frati, J. J. Rocca, V. N. Shlyaptsev, and A. L. Osterheld, Phys. Rev. E **65**, 026404 (2002).
[14] A. Rahman, E. C. Hammarsten, S. Sakadic, J. J. Rocca, and J.-F. Wyart, Phys. Scr. **67**, 414 (2003).
[15] C. D. Macchietto, B. R. Benware, and J. J. Rocca, Opt. Lett. **24**, 1115 (1999).
[16] H. Fiedorowicz, A. Bartnik, Y. Li, P. Lu, and E. Fill, Phys. Rev. Lett. **76**, 415 (1996).
[17] P. Lu *et al.*, Opt. Lett. **27**, 1911 (2002).
[18] P. Bogen, H. Conrads, G. Gatti, and W. Kohlhaas, J. Opt. Soc. Am. **58**, 203 (1968).
[19] R. A. McCorkle, Appl. Phys. A **26**, 261 (1981).
[20] R. L. Shepherd, D. R. Kania, and L. A. Jones, Phys. Rev. Lett. **61**, 1278 (1988).
[21] Y. Ehrlich, C. Cohen, A. Zigler, J. Krall, P. Sprangle, and E. Esarey, Phys. Rev. Lett. **77**, 4186 (1996).
[22] M. A. Kloshner and W. T. Silfvast, Opt. Lett. **23**, 1609 (1998).
[23] Y. Wang, B. M. Luther, M. Berrill, M. Marconi, F. Brizuela, J. J. Rocca, and V. N. Shlyaptsev, Phys. Rev. E **72**, 026413 (2005).
[24] P. Choi and M. Favre, Rev. Sci. Instrum. **69**, 3118 (1998).
[25] I. Krisch, P. Choi, J. Larour, M. Favre, J. Rous, and C. Leblanc, Contrib. Plasma Phys. **40**, 135 (2000).
[26] V. N. Shlyaptsev, J. J. G. Rocca, and A. L. Osterheld, Proc. SPIE Int. Soc. Opt. Eng. **2520**, 365 (1995).
[27] M. Klapisch, M. Busquet, and A. Bar-Shalom, AIP Conf. Proc. **926**, 206 (2007).
[28] See Supplemental Material at http://link.aps.org/supplemental/10.1103/PhysRevLett.114.095001 for details on the experimental setup and heating mechanism computations.
[29] F. B. Rozmej and O. N. Rozmej, J. Phys. B **29**, L359 (1996).
[30] U. Feldman, G. A. Doschek, D. J. Nagel, R. D. Cowan, and R. R. Whitlock, Astron. J. **192**, 213 (1974).
[31] A. H. Gabriel, Mon. Not. R. Astron. Soc. **160**, 99 (1972).